UA62784, a novel inhibitor of centromere protein E kinesin-like protein

Meredith C. Henderson,[1] Yeng-Jeng Y. Shaw,[2] Hong Wang,[4] Haiyong Han,[4] Laurence H. Hurley,[1,2,3] Gary Flynn,[2] Robert T. Dorr,[1,3] and Daniel D. Von Hoff[4]

[1]Arizona Cancer Center, [2]BIO5 Institute, and [3]College of Pharmacy, University of Arizona, Tucson, Arizona and [4]Translational Genomics Research Institute, Phoenix, Arizona

Abstract

Pancreatic carcinoma is the fourth leading cause of death from cancer. Novel targets and therapeutic options are needed to aid in the treatment of pancreatic cancer. The compound UA62784 is a novel fluorenone with inhibitory activity against the centromere protein E (CENP-E) kinesin-like protein. UA62784 was isolated due to its selectivity in isogenic pancreatic carcinoma cell lines with a deletion of the DPC4 gene. UA62784 causes mitotic arrest by inhibiting chromosome congression at the metaphase plate likely through inhibition of the microtubule-associated ATPase activity of CENP-E. Furthermore, CENP-E binding to kinetochores during mitosis is not affected by UA62784, suggesting that the target lies within the motor domain of CENP-E. UA62784 is a novel specific inhibitor of CENP-E and its activity suggests a potential role for antimitotic drugs in treating pancreatic carcinomas. [Mol Cancer Ther 2009;8(1):36–44]

Introduction

Pancreatic carcinoma is the fourth leading cause of cancer-related deaths in the United States today (1). Most patients are diagnosed with advanced disease at a time when very little can be done to extend life expectancy beyond 5 to 6 months in inoperable cases (for review, see ref. 2). Gemcitabine (Gemzar) remains the best treatment option, although it only modestly increases survival (3, 4). The antimitotic agent docetaxel has been used as a potential adjuvant treatment for pancreatic carcinoma, although clinical results comparing gemcitabine-docetaxel combination to gemcitabine alone have been mixed (5–7). Recent work shows that the mitotically active Aurora kinase is overexpressed and may comprise a potential target in pancreatic cancer (8). Indeed, the anti-Aurora kinase drug VX-680 shows potent, selective cytotoxicity and suppression of pancreatic tumor growth in xenografted mice (9). These findings provide support for the use of novel antimitotic agents in treating pancreatic carcinoma.

During mitosis, paired homologous chromosomes are segregated into two daughter cells through attachment to a bipolar spindle. The formation of a functional bipolar spindle is absolutely essential to the equitable division of genetic material and failure to form such a structure leads to mitotic arrest and cell death (for review, see ref. 10). The spindle checkpoint monitors both the attachment of microtubules to the kinetochores and the tension exerted by these attachments (11–13). Only when all kinetochores are attached to opposing poles can anaphase proceed and thereby allow division of the duplicated chromosomes. Agents that prevent this mitotic process from proceeding are referred to as mitotic inhibitors or antimitotic agents.

Mitotic inhibitors, such as taxanes and *Vinca* alkaloids, have proven to be extremely useful in the treatment of various cancers. However, it is worth noting that the vast majority of mitotic inhibitors target microtubule polymerization and most produce limiting side effects such as neurotoxicity and neutropenia (14, 15). Additionally, many of these agents are subject to acquired drug resistance usually through P-glycoprotein-mediated extrusion of drug from the cell (15, 16). Recently, the requisite involvement of other mitotic factors [polo-like kinase 1 (17), Aurora A kinase (8), and Eg5 kinesin (18)] have sparked interest as potential targets for drug development, especially in developing antimitotic agents that do not target microtubules (for review, see ref. 19).

Recently, monastrol was introduced as a mitotic inhibitor that does not affect tubulin polymerization rather; it blocks mitosis by inhibiting Eg5 kinesin ATPase activity (20). Monastrol is highly selective for the Eg5 kinesin and is effective in the low nanomolar range (20, 21). Additionally, Eg5 has been validated as a molecular target for treatment of various cancers (22–24). Monastrol was the first example of a targeted Eg5 inhibitor. Before monastrol, most previously known kinesin inhibitors affected multiple kinesin family members (25). The mitotic kinesin motor proteins such as Eg5 and centromere protein E (CENP-E) are of interest because they are only involved in mitosis and not in neuronal function. CENP-E is a kinesin-like protein that localizes to the kinetochore during mitosis and is essential for bipolar spindle formation (26, 27). The ability of CENP-E to capture microtubules and its association with BubR1 are thought to play a major role in the spindle checkpoint (28). Cells treated with small interfering RNA or

Received 6/16/08; revised 10/20/08; accepted 11/12/08.

Grant support: NIH Pancreatic Program Project grant CA109552 and CA023074.

The costs of publication of this article were defrayed in part by the payment of page charges. This article must therefore be hereby marked *advertisement* in accordance with 18 U.S.C. Section 1734 solely to indicate this fact.

Requests for reprints: Robert T. Dorr, Arizona Cancer Center, University of Arizona, 1515 North Campbell Avenue, Tucson, AZ 85724-5024. Phone: 520-626-7892; Fax: 520-626-2751. E-mail: bdorr@azcc.arizona.edu

doi:10.1158/1535-7163.MCT-08-0789

injected with antibodies against CENP-E arrest before metaphase (27, 29, 30).

The small-molecule UA62784 was isolated from a high-throughput cytotoxicity screen of a commercially available Nanosyn-based chemical library. The goal was to isolate compounds that selectively targeted DPC4-deleted pancreatic cancer cells (31). Although known to be cytotoxic in the nanomolar range, the mechanism of action for UA62784 was heretofore unknown. We report here that UA62784 causes reversible cell cycle arrest in mitosis before metaphase, with treated cells failing to form a functional bipolar spindle. Treated cells undergo apoptosis, and although UA62784 prevents the formation of a functional bipolar spindle, it does not affect tubulin polymerization nor does it affect certain signal transduction events before activation of the anaphase-promoting complex. Finally, we will show that UA62784 causes mitotic arrest by inhibiting the microtubule-associated ATPase activity of the CENP-E kinesin-like protein.

Materials and Methods

UA62784 Synthesis

To obtain sufficient amounts of drug for biological testing, a chemical synthesis of UA62784 was carried out (Fig. 1). A solution of 9-oxo-9H-fluorene-4-carboxylic acid (11.21 g, 50.0 mmol) in 150 mL DCM thionyl chloride (11.90 g, 100.0 mmol), and DMF (0.366 g, 5.0 mmol) was stirred at reflux for 2 h and evaporated *in vacuo* to remove excess amount of thionyl chloride. The solid residue was dissolved in 200 mL DCM, 2-amino-4′-methoxyacetophenone hydrochloride (8.07 g, 90% purity, 40.0 mmol) was added to the solution and triethylamine (10.12 g, 100.0 mmol) was added in portions to the ice-bath solution. The mixture was allowed to stir at room temperature for 18 h. The solution solvent was evaporated *in vacuo* and ethyl ether (100 mL) was added to the residue. The solution was filtered and washed with water, 1 N NaOH, 1 N HCl, and water. The solid was successively washed with DCM and ethyl acetate to obtain UA62784 amide (12.7 g, 34.2 mmol, 68.4% yield). ^{1}H NMR ($CDCl_3$) 3.94 (s, 3 H), 5.02 (d, J = 4.5 Hz, 2 H), 7.03 (d, J = 9.0 Hz, 2 H), 7.16 (brs, 1 H, NH), 7.34-7.50 (m, 3 H), 7.64 (d, J = 7.8 Hz, 1 H), 7.72 (d, J = 7.5 Hz, 1 H), 7.79 (d, J = 7.5 Hz, 1 H), 7.87 (d, J = 8.1 Hz, 1 H), 8.05 (d, J = 9.0 Hz, 2 H) ppm.

Phosphorus oxychloride (12.39 g, 81.0 mmol) was added dropwise to a solution of UA62784 amide (10.0 g, 26.9 mmol) in DMF (200 mL). The mixture was heated to 90°C for 30 min and then poured into iced water (200 mL). The solution was extracted with DCM (200 mL) and combined organic phases were washed with water and brine, dried, and concentrated and washed with 20% DCM in hexane to obtain UA62784 (6.74 g, 19.07 mmol, 70.8% yield) as a yellow solid. ^{1}H NMR ($CDCl_3$) 3.89 (s, 3 H), 7.02 (d, J = 8.7 Hz, 2 H), 7.36-7.52 (m, 4 H), 7.71 (d, J = 9.0 Hz, 2 H), 7.75 (d, J = 7.5 Hz, 1 H), 7.82 (d, J = 6.5 Hz, 1 H), 8.08 (d, J = 6.9 Hz, 1 H), 8.58 (d, J = 7.8 Hz, 1 H) ppm. ^{13}C NMR (75 MHz, $CDCl_3$) 55.81, 114.96, 120.83, 122.27, 123.88, 124.53, 125.88, 126.07, 126.30, 129.29, 129.92, 134.70, 135.40, 135.99, 136.16, 142.37, 144.14, 152.25, 159.11, 160.56, 193.63 ppm. HRMS $(M + H)^+$ calculated for $C_{23}H_{16}NO_3$ 354.1130; found 354.1140.

Cell Culture

Human pancreatic adenocarcinoma cell lines (BxPC3, MiaPaCa, and Panc-1) were purchased from the American Type Culture Collection and grown in RPMI supplemented with 10% bovine calf serum (Hyclone), 50 units/mL penicillin and 50 μg/mL streptomycin (Invitrogen), and 2 mmol/L L-glutamine (Invitrogen). Human foreskin fibroblast cells were established from fresh tissues at the Arizona Cancer Center (courtesy of the tissue culture shared service at Arizona Cancer Center). All cultures were incubated at 37°C in a humidified incubator with 5% CO_2.

3-(4,5-Dimethylthiazol-2-yl)-2,5-Diphenyltetrazolium Bromide Viability Assay and Apoptosis

The 3-(4,5-dimethylthiazol-2-yl)-2,5-diphenyltetrazolium bromide assay measures mitochondrial activity in viable cells based on the ability to convert 3-(4,5-dimethylthiazol-2-yl)-2,5-diphenyltetrazolium bromide to blue formazan (32). Cultured cells were seeded onto a 96-well microtiter plate. Cells were incubated with various amounts of UA62784 for 24, 48, 72, or 96 h. At the end of the incubation, 3-(4,5-dimethylthiazol-2-yl)-2,5-diphenyltetrazolium bromide solution (thiazolyl blue tetrazolium bromide; Sigma) was added to each well at a final concentration of 0.2 mg/mL. The plates were incubated for 4 h at 37°C in a humidified incubator, centrifuged briefly, and aspirated. DMSO was added to each well to dissolve formazan crystals and allow for even color

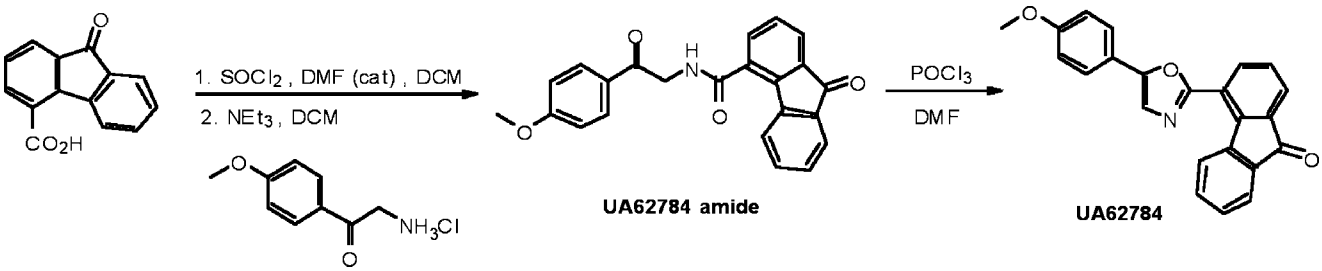

Figure 1. Synthesis of UA62784.

distribution. Absorbance was measured by a μQuant Microplate Spectrophotometer (BioTek Instruments). The IC_{50} values (defined as the drug concentration that inhibits cell growth by 50% of the control value) were determined by sigmoidal analysis using Origin 7.0 software.

To determine whether UA62784-treated cells undergo apoptosis, an Annexin V-FITC Apoptosis Detection kit (BioVision) was used. Briefly, cells were treated with UA62784 for 24 or 48 h, harvested by trypsinization, and pelleted by centrifugation. All samples were resuspended in 1× binding buffer (BioVision). Propidium iodide (PI) and Annexin V conjugated to FITC were added to each sample and samples were incubated for 5 min at room temperature. All samples were analyzed by flow cytometry using FITC signal detection and phycoerythrin emission signal detection (to detect PI).

Cell Cycle Analysis

Cells were incubated with UA62784 for 12 h. The cells were collected, washed with PBS (Invitrogen), and then fixed and permeabilized in 70% ethanol for at least 24 h at −20°C. After incubation, pellets were rehydrated and incubated with primary antibody for 1 h. Samples were then centrifuged, aspirated, and resuspended in PBS with secondary antibody for 30 min. Samples were washed as above and resuspended in PBS with 0.5 mg/mL RNase A and 0.04 mg/mL PI (Sigma). All samples were analyzed using a Becton Dickinson FACScan flow cytometer.

The mitotic index measurement procedure was modified from Muehlbauer et al. (33). Briefly, cells were treated with UA62784, demecolcine (Sigma), or doxorubicin (Sigma), incubated with anti-phospho-histone H3 and PI, and analyzed by flow cytometry as above. All primary and secondary antibodies were used at dilutions recommended by the manufacturer. Phospho-histone H3 (Ser^{10}), phospho-cdc25C (Ser^{198}), and phospho-cdc2 (Tyr^{15}) antibodies were purchased from Cell Signaling Technology.

Microscopy

Cells were seeded into chamber slides or coverslips and allowed to attach overnight. Samples were treated with UA62784 for a predetermined amount of time. Samples were fixed using either 100% methanol (tubulin samples) or 3.7% formaldehyde in PBS followed by 100% ethanol (non-tubulin samples). Samples were blocked with PBS-0.3% Triton-1% bovine calf serum.

Mouse anti-β-tubulin was purchased from Sigma. Rabbit anti-CENP-E was purchased from Cytoskeleton. Mouse anti-BubR1 was purchased from Abcam. Goat anti-mouse and goat anti-rabbit secondary antibodies were purchased from Molecular Probes/Invitrogen. All antibody incubations were done at concentrations recommended by the manufacturer. Primary antibodies were incubated overnight at 4°C and secondary antibodies were incubated for 1 to 2 h at room temperature. Slides were mounted using Vectashield Hard Set Mounting Medium with DAPI (Vector Laboratories). Confocal images were visualized using a Nikon PCM2000 microscope and SimplePCI 6.0 software (Hamamatsu).

Tubulin Polymerization Assay

Cell-free fluorescence-based tubulin polymerization kit and microtubule-associated protein (MAP) extract were purchased from Cytoskeleton. The assay was done as indicated by manufacturer. All samples (wells) were prepared with 20% glycerol, 1 mmol/L GTP, and 2 mg/mL tubulin monomers, except for MAP extract samples, which contained 5% glycerol. Paclitaxel (3 μmol/L; 4), vincristine (3 μmol/L; Sigma), and various concentrations of UA62784 were added to prewarmed plate before the addition of Tubulin Reaction Mix. The polymerization reaction was measured using a Gemini XPS Microplate Spectrofluorometer (Molecular Devices). All time points were plotted and analyzed using SoftMax Pro software (Molecular Devices).

Kinesin ATPase Assay

The colorimetric kinesin ATPase assay was purchased from Cytoskeleton and done as indicated by manufacturer. In short, purified kinesin protein (0.2-1.0 μg; Cytoskeleton) was added to paclitaxel-stabilized microtubules in a 96-well plate. Various amounts of UA62784 were added to the wells before addition of ATP (Sigma) and reaction was incubated at room temperature for 5 min. CytoPhos reagent (Cytoskeleton) was added to halt the reaction and color was allowed to develop for 10 min. Absorbance at 650 nm was measured by a μQuant Microplate Spectrophotometer (BioTek Instruments).

Microtubule Binding and PAGE

The microtubule-binding protein spin-down assay kit was purchased from Cytoskeleton and completed as indicated by manufacturer. Briefly, purified Taxol-stabilized microtubules were incubated at 37°C with microtubule-binding proteins. MAP was used as a positive control for microtubule binding and bovine serum albumin (Sigma) was used for a negative control. Test samples had 1 μg purified CENP-E motor protein (Cytoskeleton) with varying concentrations of UA62784 (0-100 μmol/L). All samples were ultracentrifuged to pellet the microtubules and aliquots were taken from the supernatant and pellet fractions.

All samples were boiled for 10 min and run on a 10% SDS polyacrylamide gel. The resulting gel was either stained with Bio-Safe Coomassie blue (Bio-Rad Laboratories) as indicated by manufacturer or transferred to an Immobilon transfer membrane (Millipore). The membrane was blocked with Odyssey Blocking Buffer (Li-Cor Biosciences), washed, and incubated with primary antibody diluted in 5% milk. Secondary antibodies were purchased from Li-Cor Biosciences. The membrane was incubated with secondary antibodies for 1 h, washed, and analyzed using an Odyssey Infrared Imager and Odyssey 2.1 software (Li-Cor Biosciences).

Results

Effects of UA62784 on Cell Survival and Apoptosis

To evaluate the *in vitro* cytotoxic activity of UA62784, we used the 3-(4,5-dimethylthiazol-2-yl)-2,5-diphenyltetrazolium bromide assay to determine the IC_{50}. MiaPaCa,

BxPC3, and Panc-1 cells were treated with various concentrations of UA62784 and incubated for 96 h. The IC_{50} value for each was calculated by sigmoidal analysis on a logarithmic curve. These results revealed varying sensitivities to UA62784 in the three cell lines, with MiaPaCa being the most sensitive (43.25 ± 4.03 nmol/L), Panc-1 being intermediate (85 ± 7.07 nmol/L), and BxPC3 being the least sensitive (103.8 ± 14 nmol/L). Overall, all three cell lines were significantly more sensitive than primary foreskin fibroblast cells (IC_{50} >> 50 μmol/L) and the lung embryonic fibroblast cell line IMR-90 (IC_{50} = 3.13 μmol/L).

All three cell lines were analyzed for evidence of apoptosis by staining with Annexin-V-FITC and PI. Pancreatic cells were incubated with varying concentrations of UA62784 for 24 or 48 h and analyzed by flow cytometry. In all cases, samples treated with ≥500 nmol/L UA62784 showed evidence of apoptosis (as opposed to necrosis, indicated by staining for PI only) at both 24 and 48 h (Supplementary Fig. S1).[5]

UA62784 Induces G_2-M Arrest

Flow cytometric analysis was used to determine the effects of UA62784 on cell cycle progression in the three pancreatic cell lines (represented in Fig. 2). The MiaPaCa cell line exhibited a consistent G_2-M arrest within 12 h incubation with 100 nmol/L UA62784. The BxPC3 and Panc-1 cell lines also exhibited a G_2-M arrest but required treatment with 300 nmol/L UA62784 for 12 h before G_2-M arrest was visible. Interestingly, treatment beyond 24 h resulted in varying responses from the three cell lines. A high sub-G_1 peak in MiaPaCa cells suggests that these cells undergo cell death following prolonged drug exposure. The BxPC3 cell line subverts the cell cycle block with prolonged exposure and continues cycling; producing a 8n peak, which is visible after treating with 300 nmol/L UA62784 for 36 h. After 48 h continuous treatment, Panc-1 cells appeared to remain arrested in G_2-M, with no sub-G_1 peaks and some slight accumulation of 8n cells (no significant peaks) appearing at the highest drug concentration. In the cases of both BxPC3 and MiaPaCa cells, the G_1 peak completely disappeared following prolonged incubation with UA62784. Prolonged incubation in Panc-1 cells resulted in the G_1 peak dropping from 56.2% (control) to 8.7% (300 nmol/L UA62784 for 36 h).

The G_2-M arrest induced by UA62784 is readily reversible over time as evidenced in Fig. 2. The MiaPaCa cells were treated with 100 nmol/L UA62784 for 8 h, enough to cause a G_2-M arrest but not to cause apoptosis (Supplementary Fig. S1).[5] These cells were then washed and allowed to recover in normal medium for various amounts of time. After 1 h recovery, the G_2-M peak had dropped significantly and appeared to have completely returned to a normal cell cycle distribution after only 3 h recovery.

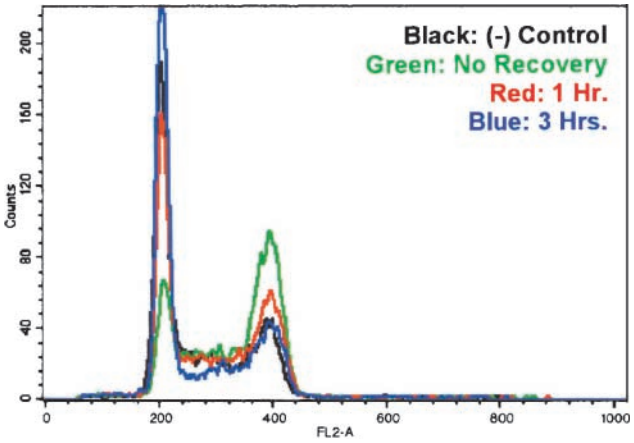

Figure 2. Flow cytometric cell cycle analysis following recovery from UA62784 treatment. MiaPaCa cells were treated with UA62784 for 8 h and allowed to recover in fresh medium for the indicated amount of time. Cells were harvested, incubated with PI, and analyzed by flow cytometry. Results show a loss of G_2-M accumulation (*far right peak*) and a gain of the G_1 population (*left peak*) over time.

Delineating the Arrest Stage, G_2-M

The flow cytometry experiments could not delineate if UA62784 was causing cell cycle arrest in the G_2 or mitotic phase because total DNA content is the same for these two phases. Therefore, the expression of phospho-histone H3 (Ser^{10}), a well-established mitotic marker (34), was examined by flow cytometry and fluorescence microscopy. Mitotic cells were defined as those with a 4n DNA content and positive staining for phospho-histone H3.

MiaPaCa cells were treated for 8 h with various amounts of UA62784 (Fig. 3A). The mitotic population begins increasing at 100 nmol/L and peaks at 500 μmol/L. Cells were also treated with demecolcine (a colchicine analogue and known tubulin polymerization inhibitor; Fig. 3B) and doxorubicin (Fig. 3C) to serve as positive and negative controls for mitotic inhibition, respectively. Demecolcine produced a substantial increase in the mitotic population as expected, whereas treatment with doxorubicin (a topoisomerase II inhibitor) caused a decrease in the mitotic population. This was expected because doxorubicin is known to inhibit cells in G_1-G_2 (35). Both Panc-1 and BxPC3 cells exhibited similar results showing arrest in early mitosis after exposure to UA62784 (data not shown).

To confirm these results, fluorescence microscopy was done using the same phospho-histone H3 marker (Supplementary Fig. S2).[5] Untreated cells showed only a small percentage of the total population in mitosis (7.6 ± 1.7%). Additionally, all stages of mitosis were seen in untreated samples. Following treatment with UA62784, the mitotic population was significantly enriched (41.5 ± 4.9%). Interestingly, it appeared that none of the treated cells had progressed into metaphase as evidenced by a lack of chromosomal alignment at the metaphase plate. All of the treated cells that were in mitosis appeared to be in either prophase or prometaphase as evidenced by the presence of

[5] Supplementary material for this article is available at Molecular Cancer Therapeutics Online (http://mct.aacrjournals.org/).

condensed chromatin or lack thereof. Additionally, cells treated with UA62784 lacked a bipolar spindle. We therefore concluded that UA62784 causes mitotic arrest before metaphase.

UA62784 Does Not Directly Influence Tubulin Polymerization

Due to the lack of a functional mitotic spindle in UA62784-treated cells (Supplementary Fig. S3),[5] we sought to determine if UA62784 affects tubulin polymerization. For this, we used a cell-free tubulin polymerization assay that relies on a fluorescence-based reporter system. Paclitaxel and vincristine were used as positive and negative controls, respectively. As shown in Supplementary Fig. S4,[5] UA62784 does not significantly affect tubulin polymerization, but the positive controls produced classic hyperpolymerization (paclitaxel) or blocked polymerization (vincristine).

MAPs are proteins that bind to tubulin to assist in polymerization and stabilization (36). Because inhibition of MAPs might have the same overall affect as a direct

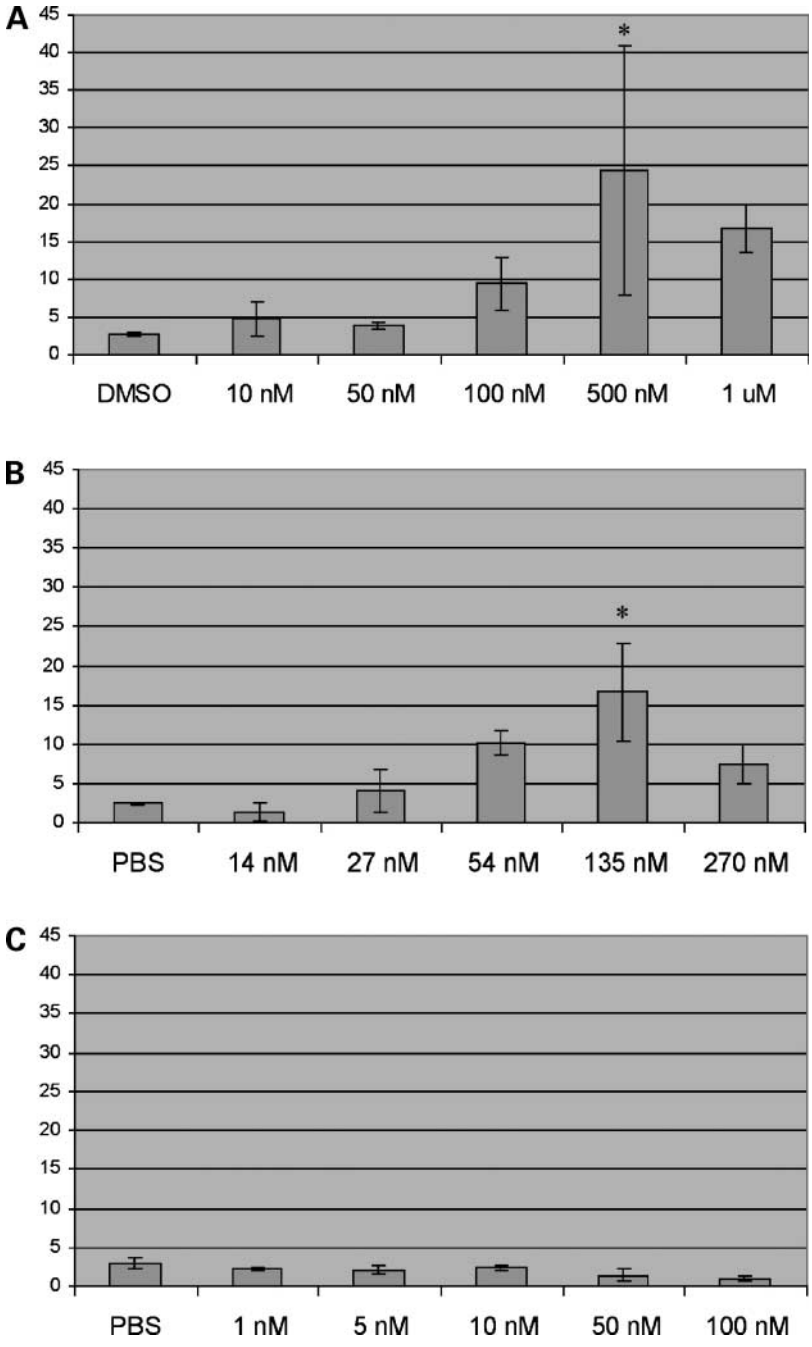

Figure 3. Mitotic index in cells treated with UA62784. Cells were incubated with the indicated amounts of UA62784 for 8 h (**A**), demecolcine for 24 h (**B**), or doxorubicin for 12 h (**C**). Cells were harvested and incubated with an anti-phospho-histone H3 antibody and PI. Samples were analyzed by flow cytometry to quantify the mitotic index as indicated by a 4n DNA content and positive staining for phospho-histone-H3. *Bars,* SD (n = 3; **A** and **B**). *, P = 0.05, statistically significant results.

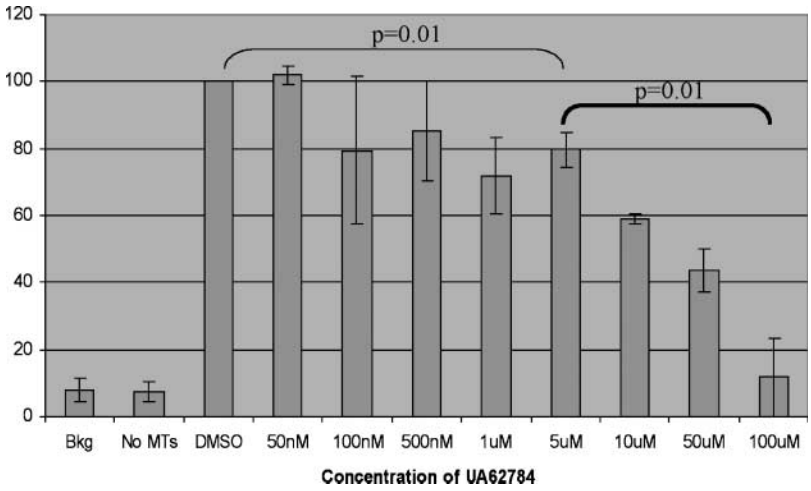

Figure 4. Kinesin ATPase assay using CENP-E purified motor domain protein. ATPase activity was measured by generation of Pi following addition of ATP and Taxol-stabilized microtubules to purified kinesin motor protein. *Bkg,* background; no ATP added, No microtubules- no microtubules added to reaction, DMSO-negative control, no UA62784 added. *Bars,* SD (n = 4).

inhibition of tubulin, we repeated the tubulin polymerization assay with a MAP fraction added (which includes MAP1, MAP2, and τ proteins). Again, tubulin polymerization assisted by MAPs was not significantly affected by the addition of UA62784 (data not shown).

CENP-E ATPase Activity and Localization

We next tested UA62784 for kinesin motor protein inhibition using a cell-free assay that relies on the formation of free inorganic phosphate following ATPase activity (37). Several kinesins were tested for UA62784-mediated inhibition, including Eg5, CENP-E, MKLP-1, KIF3C, and MCAK. Of these kinesins, UA62784 exhibited activity against only CENP-E, showing ~80% inhibition at the highest concentration tested (Fig. 4).

We used immunofluorescence microscopy to visualize CENP-E localization in treated versus untreated cells (Fig. 5). Untreated Panc-1 cells show a characteristic staining pattern (30), wherein CENP-E staining is absent in interphase cells but localizes to the cytoplasm during prophase, to the kinetochores during prometaphase/metaphase, and to the spindle midzone during anaphase. Cells treated with UA62784 showed both prophase-type and prometaphase-type staining with CENP-E localizing to the cytoplasm and kinetochores, respectively. However, all treated cells appeared to have kinetochores that were scattered throughout the nucleus as opposed to lining up at the metaphase plate, confirming our results that UA62784 arrests cells before metaphase.

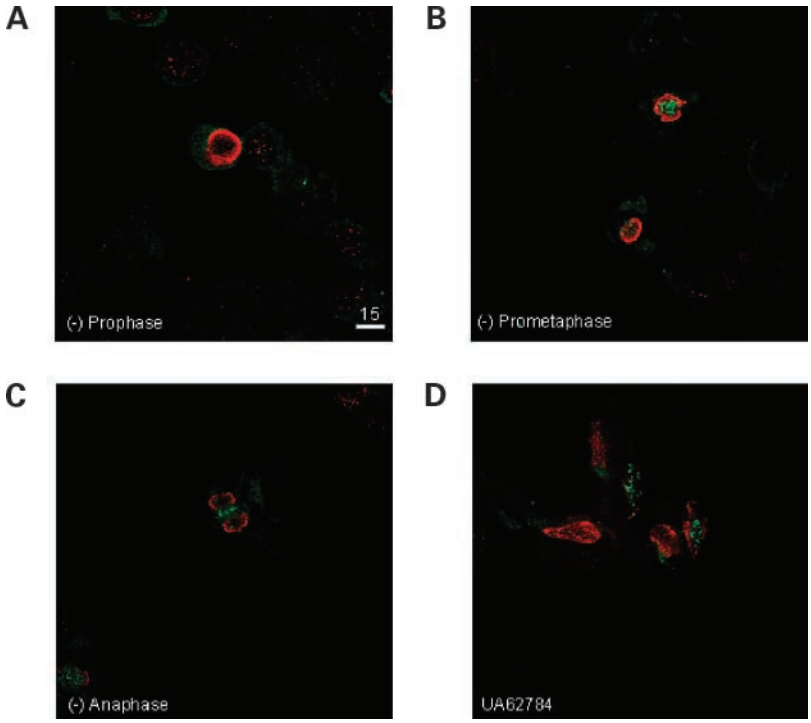

Figure 5. Immunofluorescent confocal microscopy (×40) staining for phospho-histone H3 (*red*), a mitotic marker, and CENP-E (4). Panc-1 cells were left untreated (**A**-**C**) or treated with 500 nmol/L UA62784 for 12 h. **D,** progression through mitosis, with CENP-E localizing diffusely in the cytoplasm during prophase (**A**), localizing to the DNA/kinetochores during prometaphase/metaphase (**B**), and localizing to the spindle midzone during anaphase (**C**). All cells in **A** to **C** are representative of one untreated sample. Note: only one cross-section of each confocal image is shown. Representative of three independent trials.

Because the kinesin inhibitor adociasulfate-2 acts by preventing kinesin motor binding to microtubules (25, 38), we sought to determine if UA62784 acts by a similar mechanism. A microtubule pull-down assay was done to visualize CENP-E binding in the presence and absence of UA62784 (Fig. 6). Proteins that bind to microtubules should be apparent in the pellet portion of each sample when subjected to PAGE analysis. MAP fraction and bovine serum albumin were used as positive and negative controls, respectively, for microtubule binding. When run on a PAGE gel and stained with Coomassie blue, we see that MAP fraction proteins appear in the pellet fraction, whereas bovine serum albumin appears in the supernatant fraction. Adding increasing amounts of UA62784 did not alter the amount of CENP-E within the pellet fraction; therefore, we conclude that UA62784 does not affect CENP-E binding to microtubules.

The CENP-E kinesin is known to associate with BubR1 at unattached kinetochores to facilitate spindle checkpoint signaling (39, 40). To determine if UA62784 affects the colocalization of BubR1 and CENP-E at the kinetochore during mitosis, we treated Panc-1 cells with 500 nmol/L UA62784 or an equal volume of DMSO. As shown in Supplementary Fig. S5,[5] both control and treated cells show colocalization of BubR1 and CENP-E, indicating that UA62784 does not affect the association of CENP-E and BubR1 at the kinetochore.

Discussion

These results show that UA62784 induces mitotic arrest and apoptosis in pancreatic carcinoma cell lines. Although this compound was originally isolated from a screen designed to identify compounds that would selectively target DPC4-deleted cells, it should be noted that, of the cell lines used in our experiments, only BxPC3 cells have the DPC4 gene deletion. Both MiaPaCa and Panc-1 cells have a wild-type DPC4 gene. Therefore, DPC4 status alone does not seem to directly correlate with sensitivity to UA62784. However, there was an increase in the percentage of apoptotic cells in BxPC3 ($DPC4^-$) versus BxPC3 ($DPC4^+$) cells treated with UA62784 (data not shown), confirming the initial modest selectivity for $DPC4^-$ cells. Additionally, we noticed that UA62784 has greater cytotoxic potency in pancreatic carcinoma cell lines when compared with normal fibroblast cells.

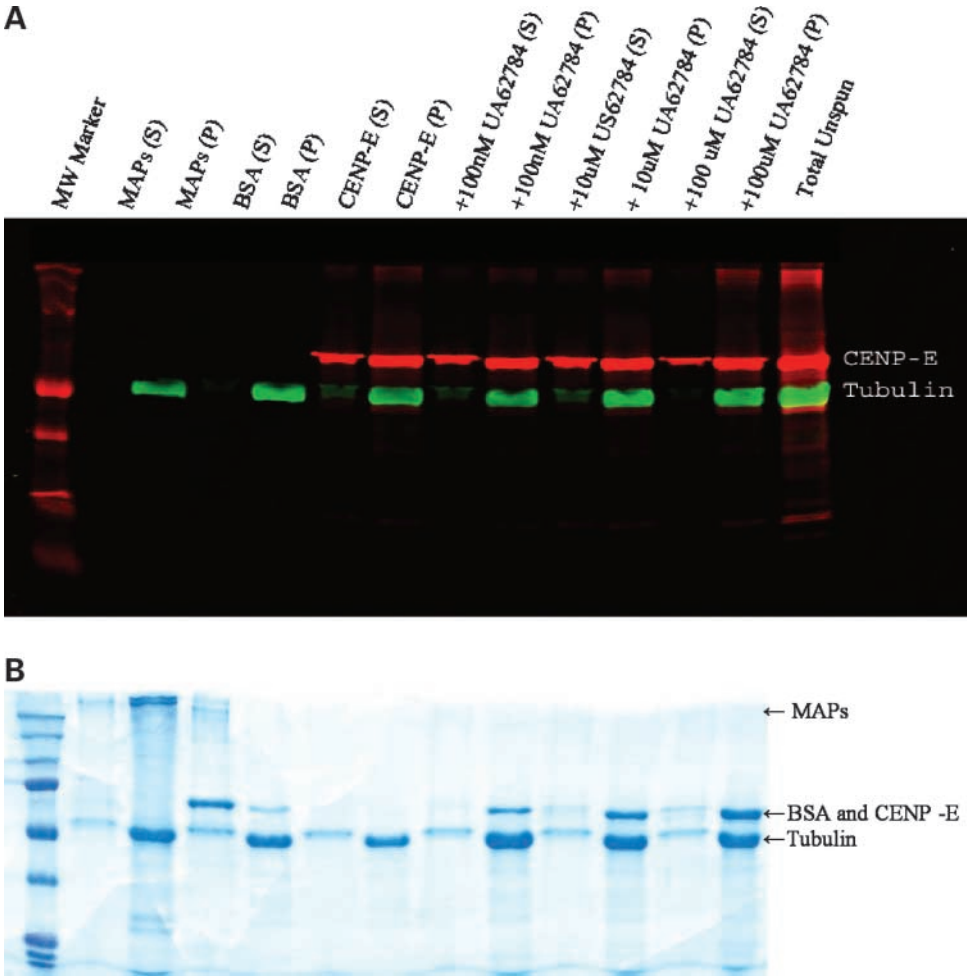

Figure 6. CENP-E microtubule-binding assay in the presence of UA62784. Purified Taxol-stabilized microtubules were incubated with MAP extract (*lanes 2-3*), bovine serum albumin (*lanes 4* and *5*), CENP-E (*lanes 6* and *7*), or CENP-E and indicated concentrations of UA62784 (*lanes 8-13*) and ultracentrifuged to pellet microtubules. Any proteins that bind microtubules would be found primarily in the pellet (*P*) fraction, whereas proteins that do not bind microtubules would be found primarily in the supernatant (*S*) fraction. Blots were visualized using IR secondary antibodies (**A**) to indicate CENP-E and tubulin proteins only and Coomassie blue staining (**B**) to indicate total protein. Representative of four independent experiments.

The mitotic arrest seen in these pancreatic cancer cell lines can be explained by the inhibition of an essential mitotic protein. Specifically, UA62784 acts on the CENP-E kinesin-like protein by inhibiting its microtubule-associated ATPase activity. Conversely, the agent does not affect the ability of CENP-E to bind to microtubules nor its localization in the mitotic cell. Inhibition of CENP-E is known to cause mitotic arrest before metaphase due to lack of chromosomal congression at the metaphase plate. Cells treated with UA62784 were viewed using immunofluorescent confocal microscopy and were seen to be arrested in either prophase or prometaphase but almost never in metaphase or anaphase. This is consistent with studies showing that the depletion of CENP-E is known to cause aneuploidy in some models (41). Indeed, we saw evidence of 8n populations in both MiaPaCa and BxPC3 cells when screening for UA62784 effects on total DNA content using flow cytometry (data not shown).

When screened against a panel of five different kinesin motor proteins, UA62784 showed inhibition of ATPase activity only in the CENP-E motor protein. Although there appears to be some disparity between the *in vitro* IC_{50} for UA62784 and the concentration required for inhibition of the purified protein, we note that previous trials with the kinesin ATPase assay required similar increases in drug concentration to elicit measurable ATPase inhibition (37). This is likely due to the fact that CENP-E kinesin protein concentrations in the cell are significantly lower than that required for the assay (42).

Although UA62784 holds promise in treating certain types of pancreatic (and presumably other) cancers, further analogue development is probably needed due to its lack of aqueous solubility. Also, we believe that a more broad-spectrum mitotic kinesin inhibitor may impart better tumor inhibition due to the redundancy seen in the function of some mitotic kinesins. These studies can be optimized to isolate compounds specific only for mitotic kinesins (such as Eg5 and CENP-E) and not neuronal kinesins (such as KIF3C). We have already developed several chemical analogues of UA62784 with improved aqueous solubility and are working to further characterize the kinesin inhibition patterns for possible clinical development. Several other kinesin inhibitors developed by other groups are currently being evaluated for clinical antitumor efficacy including two KSP/Eg5 kinesin inhibitors ispinesib (43, 44) and SB-743921 (45). To date, these inhibitors have shown limited efficacy in the clinic, underscoring the importance for continued development of alternative mitotic kinesin inhibitors that target molecules other than EG5.

Disclosure of Potential Conflicts of Interest

The authors reported no potential conflicts of interest.

References

1. Jemal A, Siegel R, Ward E, et al. Cancer statistics, 2008. CA Cancer J Clin 2008;58:71 – 96.
2. Zalatnai A. Novel therapeutic approaches in the treatment of advanced pancreatic carcinoma. Cancer Treat Rev 2007;33:289 – 98.
3. Carmichael J, Fink U, Russell RC, et al. Phase II study of gemcitabine in patients with advanced pancreatic cancer. Br J Cancer 1996;73:101 – 5.
4. Burris HA III, Moore MJ, Andersen J, et al. Improvements in survival and clinical benefit with gemcitabine as first-line therapy for patients with advanced pancreas cancer: a randomized trial. J Clin Oncol 1997;15: 2403 – 13.
5. Cascinu S, Gasparini G, Catalano V, et al. A phase I-II study of gemcitabine and docetaxel in advanced pancreatic cancer: a report from the Italian Group for the Study of Digestive Tract Cancer (GISCAD). Ann Oncol 1999;10:1377 – 9.
6. Jacobs AD. Gemcitabine-based therapy in pancreas cancer: gemcitabine-docetaxel and other novel combinations. Cancer 2002;95:923 – 7.
7. Ridwelski K, Fahlke J, Kuhn R, et al. Multicenter phase-I/II study using a combination of gemcitabine and docetaxel in metastasized and unresectable, locally advanced pancreatic carcinoma. Eur J Surg Oncol 2006;32: 297 – 302.
8. Gopalan G, Chan CS, Donovan PJ. A novel mammalian, mitotic spindle-associated kinase is related to yeast and fly chromosome segregation regulators. J Cell Biol 1997;138:643 – 56.
9. Harrington EA, Bebbington D, Moore J, et al. VX-680, a potent and selective small-molecule inhibitor of the Aurora kinases, suppresses tumor growth *in vivo*. Nat Med 2004;10:262 – 7.
10. Rudner AD, Murray AW. The spindle assembly checkpoint. Curr Opin Cell Biol 1996;8:773 – 80.
11. Pinsky BA, Biggins S. The spindle checkpoint: tension versus attachment. Trends Cell Biol 2005;15:486 – 93.
12. Rieder CL, Schultz A, Cole R, Sluder G. Anaphase onset in vertebrate somatic cells is controlled by a checkpoint that monitors sister kinetochore attachment to the spindle. J Cell Biol 1994;127:1301 – 10.
13. Li X, Nicklas RB. Mitotic forces control a cell-cycle checkpoint. Nature 1995;373:630 – 2.
14. Gotaskie GE, Andreassi BF. Paclitaxel: a new antimitotic chemotherapeutic agent. Cancer Practice 1994;2:27 – 33.
15. Zhou XJ, Rahmani R. Preclinical and clinical pharmacology of *Vinca* alkaloids. Drugs 1992;44:66 – 9.
16. Roy SN, Horwitz SB. A phosphoglycoprotein associated with Taxol resistance in J774.2 cells. Cancer Res 1985;45:3856 – 63.
17. Golsteyn RM, Mundt KE, Fry AM, Nigg EA. Cell cycle regulation of the activity and subcellular localization of Plk1, a human protein kinase implicated in mitotic spindle function. J Cell Biol 1995;129:1617 – 28.
18. Sawin KE, LeGuellec K, Philippe M, Mitchison TJ. Mitotic spindle organization by a plus-end-directed microtubule motor. Nature 1992;359: 540 – 3.
19. Miglarese MR, Carlson RO. Development of new cancer therapeutic agents targeting mitosis. Expert Opin Investig Drugs 2006;15:1411 – 25.
20. Mayer TU, Kapoor TM, Haggaarty SJ, King RW, Schreiber SL, Litchison TJ. Small molecule inhibitor of mitotic spindle bipolarity identified in a phenotype-based screen. Science 1999;286:971 – 4.
21. Kapoor TM, Mayer TU, Coughlin ML, Mitchison TJ. Probing spindle assembly mechanisms with monastrol, a small molecule inhibitor of the mitotic kinesin, Eg5. J Cell Biol 2000;150:975 – 88.
22. Koller E, Propp S, Zhang H, et al. Use of a chemically modified antisense oligonucleotide library to identify and validate Eg5 (kinesin-like 1) as a target for antineoplastic drug development. Cancer Res 2006; 66:2059 – 66.
23. Carter BZ, Mak DH, Shi Y, et al. Regulation and targeting of Eg5, a mitotic motor protein in blast crisis CML: overcoming imatinib resistance. Cell Cycle 2006;5:2223 – 9.
24. Saio T, Ishii G, Ochiai A, et al. Eg5 expression is closely correlated with the response of advanced non-small cell lung cancer to antimitotic agents combined with platinum chemotherapy. Lung Cancer 2006;54: 217 – 25.
25. Sakowicz R, Berdelis MS, Ray K, et al. A marine natural product inhibitor of kinesin motors. Science 1998;280:292 – 5.
26. Wood KW, Sakowicz R, Goldstein LSB, Cleveland DW. CENP-E is a plus end-directed kinetochore motor required for metaphase chromosome alignment. Cell 1997;91:357 – 66.
27. Schaar BT, Chan GKT, Maddox P, Salmon ED, Yen TJ. CENP-E

function at kinetochores is essential for chromosome alignment. J Cell Biol 1997;139:1373 – 82.

28. Chan GKT, Jablonski SA, Sudakin V, Hittle JC, Yen TJ. Human BUBR1 is a mitotic checkpoint kinase that monitors CENP-E functions at kinetochores and binds the cyclosome/APC. J Cell Biol 1999;146: 941 – 54.

29. Yao X, Abrieu A, Zheng Y, Sullivan KF, Cleveland DW. CENP-E forms a link between attachment of spindle microtubules to kinetochores and the mitotic checkpoint. Nat Cell Biol 2000;2:484 – 91.

30. Yen TJ, Compton DA, Wise D, et al. CENP-E, a novel human centromere-associated protein required for progression from metaphase to anaphase. EMBO J 1991;10:1245 – 54.

31. Wang H, Han H, VonHoff DD. Identification of an agent selectively targeting DPC4 (deleted in pancreatic cancer locus 4)-deficient pancreatic cancer cells. Cancer Res 2006;66:9722 – 30.

32. Mosmann T. Rapid colorimetric assay for cellular growth and survival: application to proliferation and cytotoxicity assays. J Immunol Methods 1983;65:55 – 63.

33. Muehlbauer PA, Schuler MJ. Measuring the mitotic index in chemically-treated human lymphocyte cultures by flow cytometry. Mutat Res 2003;537:117 – 30.

34. Juan G, Traganos F, James WM, et al. Histone H3 phosphorylation and expression of cyclins A and B1 measured in individual cells during their progression through G_2 and mitosis. Cytometry 1998;32:71 – 7.

35. Krishan A, Frei E III. Effect of Adriamycin on the cell cycle traverse and kinetics of cultured human lymphoblasts. Cancer Res 1976;36:143 – 50.

36. Maccioni RB, Cambiazo V. Role of microtubule-associated proteins in the control of microtubule assembly. Physiol Rev 1995;75:835 – 64.

37. Funk CJ, Davis AS, Hopkins JA, Middleton KM. Development of high-throughput screens for discovery of kinesin adenosine triphosphatase modulators. Anal Biochem 2004;329:68 – 76.

38. Brier S, Carletti E, DeBonis S, Hewat E, Lemaire D, Kozielski F. The marine natural product adociasulfate-2 as a tool to identify the MT-binding region of kinesins. Biochemistry 2006;45:15644 – 53.

39. Mao Y, Desai A, Cleveland DW. Microtubule capture by CENP-E silences BubR1-dependent mitotic checkpoint signaling. J Cell Biol 2005; 170:873 – 80.

40. Chan GK, Jablonski SA, Sudakin V, Hittle JC, Yen TJ. Human BUBR1 is a mitotic checkpoint kinase that monitors CENP-E functions at kinetochores and binds the cyclosome/APC. J Cell Biol 1999;146:941 – 54.

41. Weaver BAA, Silk AD, Montagna C, Verdier-Pinard P, Cleveland D. Aneuploidy acts both oncogenically and as a tumor suppressor. Cancer Cell 2007;11:25 – 36.

42. Brown KD, Coulson RM, Yen TJ, Cleveland DW. Cyclin-like accumulation and loss of the putative kinetochore motor CENP-E results from coupling continuous synthesis with specific degradation at the end of mitosis. J Cell Biol 1994;125:1303 – 12.

43. Lee CW, Belanger K, Rao SC, et al. A phase II study of ispinesib (SB-715992) in patients with metastatic or recurrent malignant melanoma: a National Cancer Institute of Canada Clinical Trials Group trial. Invest New Drugs 2008;26:249 – 55.

44. Blagden SP, Molife LR, Seebaran A, et al. A phase I trial of ispinesib, a kinesin spindle protein inhibitor, with docetaxel in patients with advanced solid tumours. Br J Cancer 2008;98:894 – 9.

45. O'Connor O, Goy A, Orlowski R, et al. Phase I-II study to determine the safety, pharmacokinetics and potential efficacy of the kinesin spindle protein (KSP) inhibitor SB-743921 on days 1 and 15 of a 28 day schedule in patients with non-Hodgkin's or Hodgkin's lymphoma. 49th American Society of Hematology Annual Meeting; 2007 December; Atlanta, GA.